Galectin-3 Protein Regulates Mobility of N-cadherin and GM1 Ganglioside at Cell-Cell Junctions of Mammary Carcinoma Cells*[S]

Cécile Boscher[‡], **Yu Zi Zheng**[§1], **Ramya Lakshminarayan**[¶], **Ludger Johannes**[¶2], **James W. Dennis**[||],
Leonard J. Foster[§3], and **Ivan R. Nabi**[‡4]

From the ‡*Department of Cellular and Physiological Sciences, Life Sciences Institute, University of British Columbia, Vancouver, British Columbia V6T 1Z3, Canada, the* §*Centre for High-Throughput Biology and Department of Biochemistry and Molecular Biology, University of British Columbia, Vancouver, British Columbia V6T 1Z, Canada, the* ¶*Traffic, Signaling, and Delivery Laboratory, Centre de Recherche, Institut Curie, CNRS UMR144, 26 rue d'Ulm, 75248 Paris Cedex 05, France, and the* ||*Department of Medical Genetics and Laboratory Medicine and Pathology, University of Toronto, Toronto, Ontario M5G 1L5, Canada*

Background: Galectin-3-*N*-glycan binding forms a lattice that regulates cancer cell adhesion, migration, and signaling.
Results: Galectin-3 destabilizes cell-cell junctions and increases junctional mobility of N-cadherin and GM1 ganglioside.
Conclusion: Galectin-3 is a novel regulator of N-cadherin dynamics and cell-cell junction stability.
Significance: First demonstration of galectin-3 regulation of both glycoprotein and glycolipid mobility defines novel roles for the galectin lattice in junctional stability.

Galectin-3 binding to cell surface glycoproteins, including branched *N*-glycans generated by *N*-acetylglucosaminyltransferase V (Mgat5) activity, forms a multivalent, heterogeneous, and dynamic lattice. This lattice has been shown to regulate integrin and receptor tyrosine kinase signaling promoting tumor cell migration. N-cadherin is a homotypic cell-cell adhesion receptor commonly overexpressed in tumor cells that contributes to cell motility. Here we show that galectin-3 and N-cadherin interact and colocalize with the lipid raft marker GM1 ganglioside in cell-cell junctions of mammary epithelial cancer cells. Disruption of the lattice by deletion of Mgat5, siRNA depletion of galectin-3, or competitive inhibition with lactose stabilizes cell-cell junctions. It also reduces, in a p120-catenin-dependent manner, the dynamic pool of junctional N-cadherin. Proteomic analysis of detergent-resistant membranes (DRMs) revealed that the galectin lattice opposes entry of many proteins into DRM rafts. N-cadherin and catenins are present in DRMs; however, their DRM distribution is not significantly affected by lattice disruption. Galectin lattice integrity increases the mobile fraction of the raft marker, GM1 ganglioside binding cholera toxin B subunit Ctb, at cell-cell contacts in a p120-catenin-independent manner, but does not affect the mobility of either Ctb-labeled GM1 or GFP-coupled N-cadherin in nonjunctional regions. Our results suggest that the galectin lattice independently enhances lateral molecular diffusion by direct interaction with specific glycoconjugates within the adherens junction. By promoting exchange between raft and non-raft microdomains as well as molecular dynamics within junction-specific raft microdomains, the lattice may enhance turnover of N-cadherin and other glycoconjugates that determine junctional stability and rates of cell migration.

Galectins are small β-galactoside-binding proteins that bind cell surface glycans. Although most galectins contain one or two carbohydrate domains, galectin-3 (Gal-3)[5] contains an oligomerization domain that enables oligomer formation, up to pentamers, upon binding to glycoproteins, resulting in the formation of heterogeneous cell surface lattices (1–3). The Golgi *N*-glycan branching pathway generates ligands with a range of affinities for galectins, with the higher affinities requiring *N*-acetylglucosaminyltransferase V (Mgat5) (4). Both Golgi glycan modification and the number of *N*-glycan sites encoded in the protein sequence contribute to glycoprotein affinity for galectin (5). Expression of both Mgat5 and Gal-3 has long been associated with tumor progression and metastasis (6, 7), and tumor formation is delayed in Mgat5-deficient mice (8). The affinity of tyrosine kinase receptors such as EGF or TGFβ receptors for the galectin lattice is increased by Mgat5-dependent modifications to the receptors and prevents their down-regulation by clathrin-dependent endocytosis and interaction with inhibitory caveolin-1 domains (9, 10). In T cells, the galectin lattice reduces T cell receptor clustering and recruitment to the immune synapse, thereby reducing T cell activation and autoimmunity (11–13). Gal-3 has also been proposed to restrict

[5] The abbreviations used are: Gal-3, galectin-3; DRM, detergent-resistant membrane; EGFR, epidermal growth factor receptor; Ctb, cholera toxin B subunit; FRAP, fluorescence recovery after photobleaching; DTSSP, 3,3'-dithiobis[sulfosuccinimidylpropionate]; SILAC, stable isotope labeling by amino acids in cell culture.

CD8 and T cell receptor interaction, preventing lymphocyte activation (14, 15). Mgat5 and the galectin lattice also promote focal adhesion dynamics and fibronectin fibrillogenesis, leading to enhanced matrix remodeling and tumor cell migration (16–18). A common theme is that decoding *N*-glycan modifications of cell surface receptors by the galectin lattice acts as a regulator of their turnover and membrane domain interaction (19).

Cadherins are glycoproteins responsible for homotypic and calcium-dependent cell-cell adhesion (20). α- and β-catenin are recruited to the C-terminal tail of cadherins forming a dynamic linkage with the actin cytoskeleton (21, 22). p120-catenin is a Src substrate that regulates RhoGTPase activity, which in turn promotes cadherin internalization and/or stability at the cell surface (23, 24). A key aspect of epithelial tumor cell progression is the disruption of E-cadherin-mediated cell-cell adhesions and switching to a more mesenchymal, migratory phenotype, a process called epithelial-mesenchymal transition (25). Expression of Mgat5 is associated with enhanced TGF-β receptor signaling and epithelial-mesenchymal transition (9, 10). N-cadherin (cadherin-2 or CDH-2) is a mesenchymal cadherin overexpressed in many cancers and associated with cancer cell migration and FGF receptor signaling in breast cancer metastasis (26). Mgat5-dependent glycosylation of N-cadherin has also been associated with increased cell migration and decreased cell-cell aggregation (27, 28). N- and E-cadherins have seven and three *N*-glycosylation sites, respectively, suggesting a different threshold for the galectin lattice (5). Biophysical analysis suggests that the adhesion force between N-cadherin homophilic bounds is qualitatively smaller than those of E-cadherin (29, 30), which might contribute to the lability of cell-cell contacts, thereby promoting tumor cell migration.

Here we show that Gal-3 accumulates at cell-cell junctions with N-cadherin and the raft marker ganglioside GM1 and contributes to the destabilization of cell-cell junctions. Although the sequestration of EGFR and focal adhesion proteins in the galectin lattice decreases their mobility in the plasma membrane (9, 16), the galectin lattice increases the p120-dependent mobility of N-cadherin at cell-cell junctions. The galectin lattice also enhances dynamics of GM1 ganglioside binding cholera toxin B subunit (Ctb), but not the unglycosylated raft protein flotillin-2, at cell-cell junctions independently of p120. However, although disruption of the galectin lattice results in accumulation of many proteins in detergent-resistant membranes (DRMs) or rafts, it does not impact on the raft association of cadherins and catenins. Lattice regulation of N-cadherin and Ctb mobility is specific to cell-cell junctions, and our data suggest that the galectin lattice independently regulates the dynamics of N-cadherin and GM1. Gal-3 regulation of the dynamics of N-cadherin and raft components at cell-cell junctions may play a complementary role to p120-catenin in the regulation of junctional stability and thereby tumor cell migration.

MATERIALS AND METHODS

Plasmids, Antibodies, and Reagents—Vector encoding N-cadherin-GFP was provided by Dr. Shernaz Bamji (University of British Columbia, Vancouver, Canada), and mutated N-cadherin AAA-YFP was provided by Dr René-Marc Mège (Institut du Fer à Moulin, INSERM, Paris, France). Human Gal-3 and recombinant human GST-Gal-3 was purified and coupled to Cy3 according to the manufacturer's instructions (Invitrogen). FITC-coupled Ctb and Alexa Fluor 488-, 568-, or 647-coupled anti-mouse or -rabbit or phalloidin were from Invitrogen, mouse anti-N-cadherin from BD Biosciences, rabbit anti-β-catenin was from Sigma-Aldrich, and rabbit anti-p120-catenin was from Santa Cruz Biotechnology. SMART-pool siRNA targeting Gal-3 or p120-catenin and nontargeting siRNA were from Dharmacon. Normal Dulbecco's modified Eagle's medium (DMEM) was from Sigma-Aldrich, L-glutamine, penicillin/streptomycin, BCA assay kit, and cell culture trypsin were from Invitrogen, and both qualified and dialyzed fetal bovine serum (FBS) and L-lysine- and L-arginine-deficient DMEM were from Caisson Laboratories (North Ogden, UT). Sucrose, lactose, swainsonine, L-lysine, L-arginine, Triton X-100, sodium deoxycholate, dithiothreitol (DTT), and iodoacetamide were from Sigma-Aldrich. [^{2}H$_4$]lysine, [^{13}C$_6$]arginine, [^{13}C$_6$^{15}N$_2$]lysine, and [^{13}C$_6$^{15}N$_4$]arginine were from Cambridge Isotope Laboratories. Sequencing grade modified porcine trypsin solution was from Promega, and protease inhibitor mixture tablets with EDTA were from Roche Applied Science.

Cell Culture and Transfection—Mgat5$^{+/+}$, Mgat5$^{-/-}$ and Mgat5$^{-/-\text{Res}}$ were cultured as described previously (18). Cells were plated 24 h before transfection of DNA, siRNA, or both at the same time at a ratio of 1:2 DNA:RNA using Lipofectamine 2000 in Opti-MEM (Invitrogen). Experiments were performed 48 h after transfection. Where indicated, culture medium was supplemented with 20 mM lactose, 20 mM sucrose, or 1 mM swainsonine for 48 h.

Calcium Switch Experiment and Immunofluorescence—Cells were pretreated for 48 h with 20 mM sucrose or lactose or transfected with control or Gal-3-targeted siRNA before the medium was switched to a complete medium containing only 50 μM calcium or before the addition of 1.5 mM EGTA. After 8 min for the low calcium conditions or 30 min for the EGTA treatment, cells were fixed with 3% paraformaldehyde at 37 °C and then permeabilized with 0.2% Triton X-100. After blocking in 1% BSA, cells were incubated with the primary and secondary antibodies for 1 h. Images for all conditions were acquired using equivalent settings on an Olympus FV1000 confocal microscope. Using the ImageJ image analysis software, the same threshold was applied to all N-cadherin images and, separately, to all β-catenin images based on junctional labeling in control cells. The resulting images were merged, and the Pearson's coefficient was calculated for each field. Statistical analyses were performed on GraphPad Prism 4 using an unpaired Student's *t* test (two-tailed with a confidence interval of 95%).

FRAP Analysis—Cells were plated in 8-well 15μ-Slide ibidi chambers (ibidi GmbH, Munich, Germany) 24 h before transfection. After transfection, the cells were treated, or not with 20 mM lactose or sucrose or with 1 mM swainsonine for 48 h before the experiment. Fluorescence recovery after photobleaching (FRAP) experiments were performed at 37 °C for N-cadherin-GFP and AAA-YFP and at 30 °C for FITC-coupled Ctb (9). Regions of interest, at cell-cell junctions or not, were photo-

bleached and recovery measured over time on an FV100 confocal microscope as described previously (9).

Cross-linking, Immunoprecipitation, and Western Blot Analysis—Cross-linking was performed by incubating confluent cells in 100-mm plates at 4 °C with 2 μg/ml GST-Gal-3 for 20 min before switching the medium to PBS containing 2 mM calcium and 0.1 mg/ml 3,3′-dithiobis[sulfosuccinimidylpropionate] (DTSSP, Pierce) for 1 h. After quenching, proteins were extracted in a lysis buffer containing 50 mM Tris, pH 7.5, 1 mM EDTA, 1 mM EGTA, 150 mM NaCl, 1% Triton X-100, and protease inhibitors (Roche Applied Science). Lysates were incubated with protein A-coupled Sepharose beads preincubated with 1 μg of mouse anti-N-cadherin (BD Biosciences) or 0.4 μl of rabbit anti-β-catenin (Sigma). After 2 h at 4 °C on rotator, the beads were washed in lysis buffer and suspended in loading buffer containing 25 mM DTT. 2% of the lysate used for immunoprecipitation (input) was loaded in parallel to the pulldown. Western blots were probed with HRP-coupled antibodies (Jackson ImmunoResearch) and revealed by chemiluminescence or probed with IRDye 700- or 800-conjugated antibodies (Rockland Immunochemicals) and revealed with the Odyssey imaging system (LI-COR Biosciences).

SILAC—Triplex SILAC was conducted as described previously (31). Before labeling, all Mgat5 cells were maintained in DMEM supplemented with 10% FBS (v/v), 1% L-glutamine (v/v), and 1% penicillin/streptomycin (v/v) at 5% CO_2 and 37 °C and then transferred to SILAC medium with dialyzed FBS and lysine and arginine isotopologs. To achieve complete labeling, cell populations were amplified 200-fold in the labeling media. Here we refer to the different labels as 0/0 for the normal isotopic abundance Lys and Arg, 4/6 for $[^2H_4]$Lys and $[^{13}C_6]$Arg, and 8/10 for $[^{13}C_6{}^{15}N_2]$Lys and $[^{13}C_6{}^{15}N_4]$Arg. To obtain enough material for effective proteomic analysis, five 15-cm plates of labeled Mgat5 cells were used for each of the 0/0, 4/6, and 8/10 conditions for lactose/sucrose treatment and subsequent detergent-resistant membrane extraction. In the lactose/sucrose treatment experiment, 35% confluent 0/0 and 4/6 Mgat5$^{+/+}$ cells were treated by adding 20 mM lactose or sucrose, respectively, directly to the growth medium for 48 h with 8/10 cells as the control.

DRM Preparation—DRMs were extracted from SILAC cells as described previously (31, 32). Very briefly, cells were solubilized in lysis buffer (1% Triton X-100, 25 mM 2-(*N*-morpholino)ethanesulfonic acid, pH 6.5, protease inhibitor mixture). Relative protein concentrations of cell lysates were determined using the Coomassie Plus kit (Pierce), and equal masses of protein from each SILAC condition were mixed together. From this step, lysates were combined as one sample and subjected to sucrose density gradient analysis by first mixing with an equal volume of 90% sucrose (in 25 mM MES, 150 mM NaCl, pH 6.5 (MES-buffered saline)) and then layering with 35 and 5% sucrose. These gradients were then centrifuged for 18 h at 166,000 relative centrifugal force. The white, light-scattering band appearing between 35 and 5% sucrose after centrifugation correspond to DRMs, and this was then diluted out ∼3-fold with MES-buffered saline, and membranes were further pelleted by centrifugation at 166,000 relative centrifugal force for 2 h. All steps were carried out at 4 °C.

LC-MS/MS, Database Searching, and Data Analysis—All analyses involved solution digestions in 1% sodium deoxycholate (50 mM Tris, pH 8) with protein pellets solubilized directly in sodium deoxycholate and then subjected to trypsin digestion. Protein solutions were reduced (1 μg of DTT/50 μg of protein), alkylated (5 μg of iodoacetamide/50 μg of protein), and digested (1 μg of trypsin/50 μg of protein) as described. For each sample, 5 μg (measured by the BCA method) of digested peptides were analyzed by liquid chromatography-tandem mass spectrometry (LC-MS/MS) on an LTQ Orbitrap XL (Thermo Fisher, Bremen, Germany). The LTQ Orbitrap XL was on-line-coupled to Agilent 1100 series nanoflow HPLC instruments using a nanospray ionization source (Proxeon Biosystems) holding columns packed into 15-cm-long, 75-μm-inner diameter fused silica emitters (8-μm-diameter opening, pulled on a P-2000 laser puller from Sutter Instruments) using 3-μm-diameter ReproSil Pur C18 beads. Buffer A consisted of 0.5% acetic acid, and buffer B consisted of 0.5% acetic acid and 80% acetonitrile. Gradients were run from 6% B to 30% B over 60 min and then from 30% B to 80% B in the next 10 min, held at 80% B for 5 min, and then dropped to 6% B for another 15 min to recondition the column. The LTQ Orbitrap XL was set to acquire a full range scan at 60,000 resolution from 350 to 1500 mass-to-charge units in the Orbitrap and to simultaneously fragment the top five peptide ions in each cycle in the LTQ. In all experiments, digested peptides were also further fractionated by strong cation exchange chromatography (SCX) into five fractions using 0, 20, 50, 100, and 500 mM of NH_4CH_3COO and analyzed as above on an LTQ Orbitrap XL.

Protein identification and quantification were done using Proteome Discover (v.1.2, Thermo Fisher) and Mascot (v2.3, Matrix Science) to search against the International Protein Index (IPI) Mouse (v3.69, 110,771 sequences; common serum contaminants and human keratins were added, and all reversed sequences were concatenated) database with the following criteria: electrospray ionization-ion trap fragmentation characteristics, tryptic specificity with up to one missed cleavage; ±10 ppm and ±0.6-Da accuracy for MS and MS/MS measurements, respectively; cysteine carbamidomethylation as a fixed modification; and N-terminal protein acetylation, methionine oxidation, and deamidation (Asn-Gln), triplex ($[^2H_4]$Lys, $[^{13}C_6]$Arg, $[^{13}C_6{}^{15}N_2]$Lys and $[^{13}C_6{}^{15}N_4]$Arg) SILAC modifications. Peptide false discovery rate was set at 1%. Quantitation was done using a mass precision of 2 ppm (three times the mass precision is used to create extracted ion chromatograms). After extracting each ion chromatogram, Proteome Discoverer runs several filters to check for, among other things, interfering peaks and the expected isotope pattern, and peptides that do not meet all the criteria are not used in calculating the final ratio for each protein. We consider proteins identified if at least two peptides were observed. Analytical variability of SILAC data in the types of experiments performed here is typically <20% on average, and biological variability was addressed in these experiments by performing three independent replicates of each experiment.

RESULTS

Interaction of Gal-3 and N-cadherin at Cell-Cell Junctions—Using cell lines derived from epithelial mammary tumors from Mgat5$^{+/+}$ and Mgat5$^{-/-}$ transgenic mice on a polyoma middle T (PyMT) background, we have previously shown that Mgat5 and the galectin lattice regulate EGFR signaling and focal adhesion dynamics (8–10, 16). Although Mgat5-deficient tumor cells (Mgat5$^{-/-}$ cells) retain E-cadherin expression and an epithelial phenotype, despite concomitant N-cadherin expression, Mgat5$^{+/+}$ cells and Mgat5$^{-/-}$ cells rescued by retroviral expression of Mgat5 (Mgat5$^{-/-RES}$ cells) express only N-cadherin at cell-cell junctions and have undergone epithelial-mesenchymal transition (9, 10). Incubation of Mgat5$^{+/+}$ cells with cyanine-5 (Cy5)-coupled Gal-3 at 4 °C revealed a cell surface labeling and strong accumulation of Gal-3 at cell-cell junctions where it colocalized with N-cadherin (Fig. 1*A*). Gal-3 recruitment to junctions was completely prevented by lactose treatment, which competes with cell surface glycans for Gal-3 binding, whereas control sucrose treatment does not block Gal-3 recruitment. Swainsonine inhibits Golgi α-mannosidase II, which blocks terminal *N*-glycan branching, preventing interaction with Gal-3, and blocks Gal-3 recruitment to cell-cell junctions, although a residual signal remained on the cell surface (Fig. 1*A*).

N-cadherin has been localized in rafts (33), and we also observed the localization of Ctb-FITC to cell-cell junctions, indicating an enrichment of GM1 ganglioside in these domains. Distribution of N-cadherin or Ctb at cell-cell junctions was not affected by disruption of the galectin lattice with either lactose or swainsonine (Fig. 1*A*).

To determine whether Gal-3 interacts with the N-cadherin-catenin complex at cell-cell junctions, we performed cross-linking experiments followed by N-cadherin immunoprecipitation using the membrane-impermeable DTSSP cross-linker (Fig. 1*B*). Endogenous Gal-3 is detected in the N-cadherin immunoprecipitate after cross-linking only. Untreated Mgat5$^{+/+}$ cells or sucrose-, lactose-, or swainsonine-treated cells were incubated with purified Gal-3 at 4 °C for 20 min before cross-linking. The faster migration of N-cadherin in SDS-PAGE in the swainsonine-treated cells is indicative of *N*-glycan truncation. The addition of exogenous Gal-3 strongly increases the Gal-3 signal in the N-cadherin immunoprecipitate. This enrichment is decreased by lactose and swainsonine treatment indicative of extracellular interaction of Gal-3 with N-cadherin.

To support this hypothesis, we treated the cells with 1.5 mM EGTA for 25 min before the addition of purified Gal-3 and cross-linking (Fig. 1*B*). EGTA, as a calcium chelator, is known to destabilize the extracellular domain of cadherins, resulting in loss of cell-cell adhesion and cadherin internalization (34). EGTA treatment prevents cross-linking of Gal-3 to N-cadherin, demonstrating that junctional stability is important for their interaction.

Using another approach, Mgat5$^{+/+}$ cells were incubated with GST-tagged Gal-3 (GST-Gal-3) before cross-linking and β-catenin immunoprecipitation (Fig. 1*C*). Both N-cadherin and exogenous GST-Gal-3 are detected in the β-catenin immuno-

precipitates in untreated or sucrose-treated cells but not after EGTA treatment or lattice disruption with lactose or swainsonine. In contrast to N-cadherin immunoprecipitation, endogenous Gal-3 was not detected in the β-catenin pulldown. Treatment with lactose or swainsonine reduces Gal-3-GST in both the pulldown and total extract but does not alter endogenous Gal-3 in the input. This suggests that endogenous Gal-3 may be predominantly intracellular. Interestingly, lactose treatment resulted in complete loss of Gal-3-GST in the total extract, but a reduced signal was present in swainsonine-treated cells. This suggests that residual GST-Gal-3 binds to the cell surface, possibly due to binding to *O*-glycans on glycoproteins or to glycolipids, even when *N*-glycan branching is blocked. Altogether these results suggest that Gal-3 is recruited at cell-cell junctions by direct interaction with branched *N*-glycans of N-cadherin.

Regulation of Junctional Stability of N-cadherin by the Galectin Lattice—To determine whether the galectin lattice affects cell-cell junctions, we transfected Mgat5$^{+/+}$ cells with siRNA targeting Gal-3 (supplemental Fig. S1) or treated them with sucrose, lactose, or swainsonine. Immunofluorescence analysis of N-cadherin and β-catenin colocalization revealed that these treatments did not impact on cell-cell junction formation (Fig. 2). However, when the cells were switched to low calcium medium (50 μM Ca^{2+} medium or 1.5 mM EGTA treatment), Gal-3 siRNA-, lactose-, and swainsonine-treated cells showed increased N-cadherin-β-catenin colocalization indicative of higher retention of junctional complexes when compared with untreated and sucrose-treated cells. The addition of extracellular Gal-3 did not affect cell-cell junctions in normal calcium conditions but increased junction destabilization in low calcium conditions and restored destabilization of cell-cell junctions in low calcium conditions in siGal-3-treated cells (Fig. 2*C*). This rescue effect combined with the lactose and swainsonine treatments suggests that extracellular Gal-3 destabilizes junctions, possibly by enhancing the dynamics of N-cadherin in the membrane.

We then measured the dynamic properties of N-cadherin-GFP at cell-cell junctions using FRAP (Fig. 3*A*). We observed significantly decreased recovery at junctions in lactose or swainsonine-treated and siRNA Gal-3 transfected cells in comparison with controls (Fig. 3, *B* and *C*). FRAP analysis revealed that the mobile fraction of N-cadherin was affected by lactose and swainsonine treatment but that the half-life of recovery was not significantly changed (supplemental Table S1). The effect of the galectin lattice was Mgat5-dependent as N-cadherin showed increased mobility in Mgat5$^{-/-}$ cells where its recovery was insensitive to Gal-3 siRNA and lactose treatment. Rescue of Mgat5$^{-/-}$ cells by retroviral expression of Mgat5 both increased N-cadherin mobility and restored its sensitivity to Gal-3 knockdown and lactose treatment (Fig. 3, *B* and *C*). Moreover, the effect of Gal-3 depletion was rescued by the addition of Gal-3 to the medium, indicating that extracellular Gal-3 regulates N-cadherin mobility at cell-cell junctions (Fig. 3*D*). However, we did not observe any effect of lactose on N-cadherin-GFP located in cellular lamellipodia not involved in cell-cell junctions (supplemental Fig. S2).

Next we asked whether lattice-dependent regulation of N-cadherin at cell-cell junctions was dependent on p120-
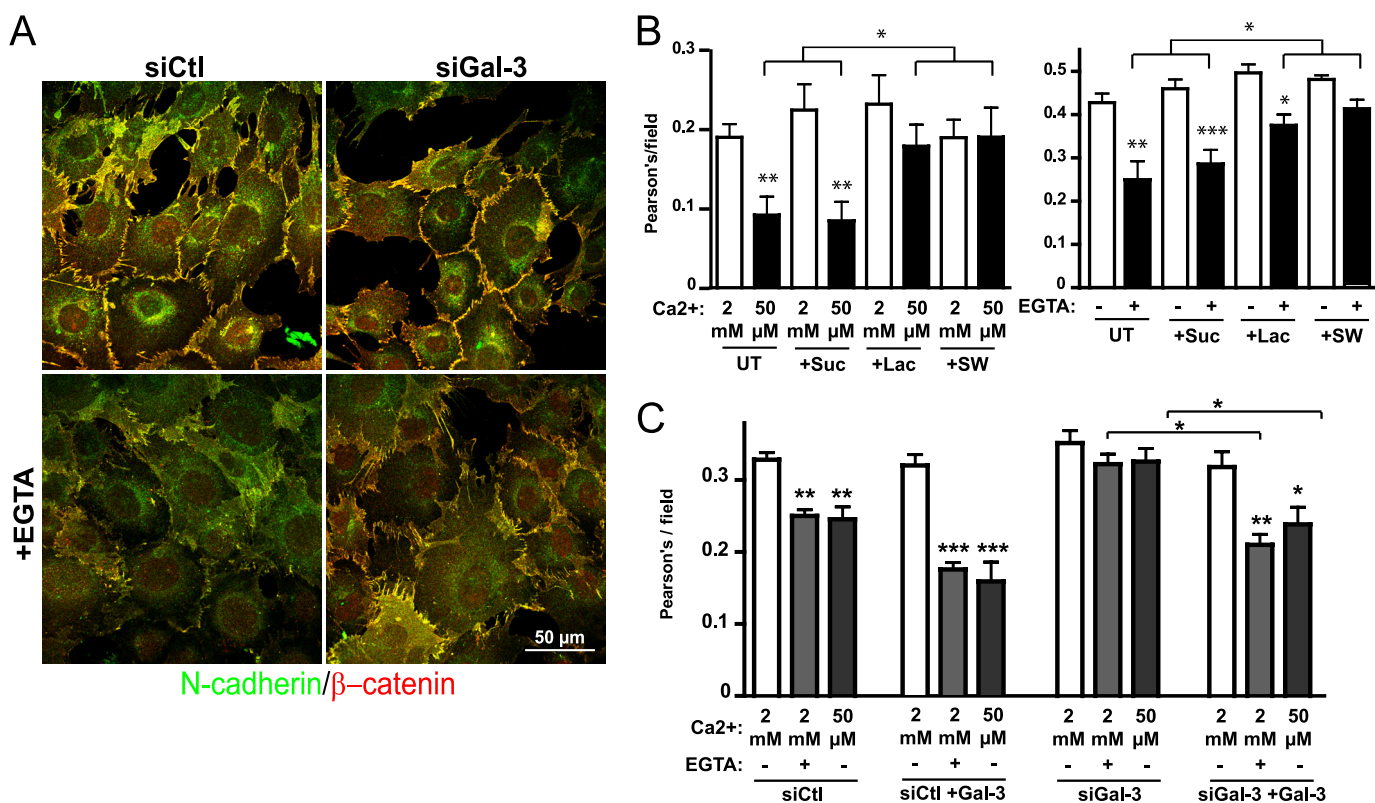
A

B

C
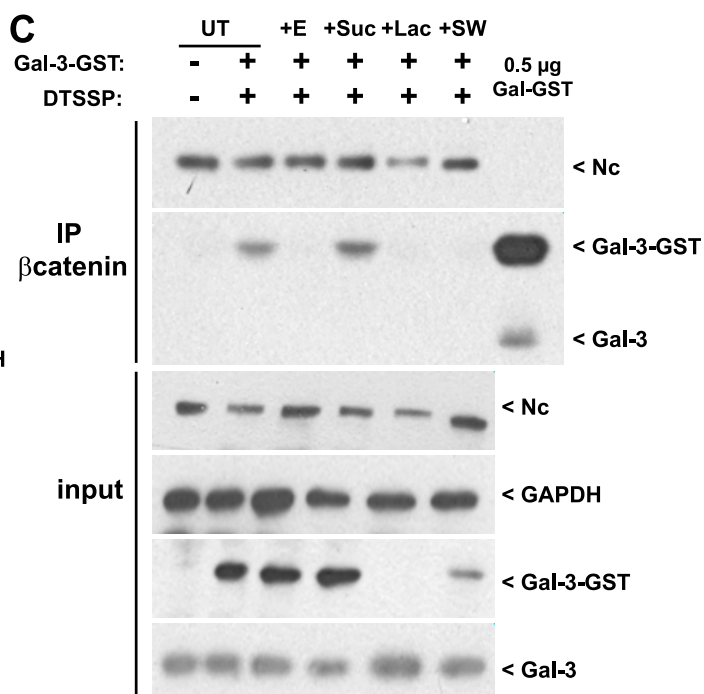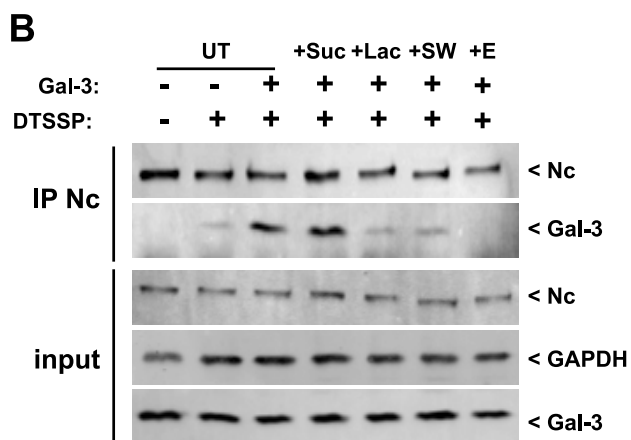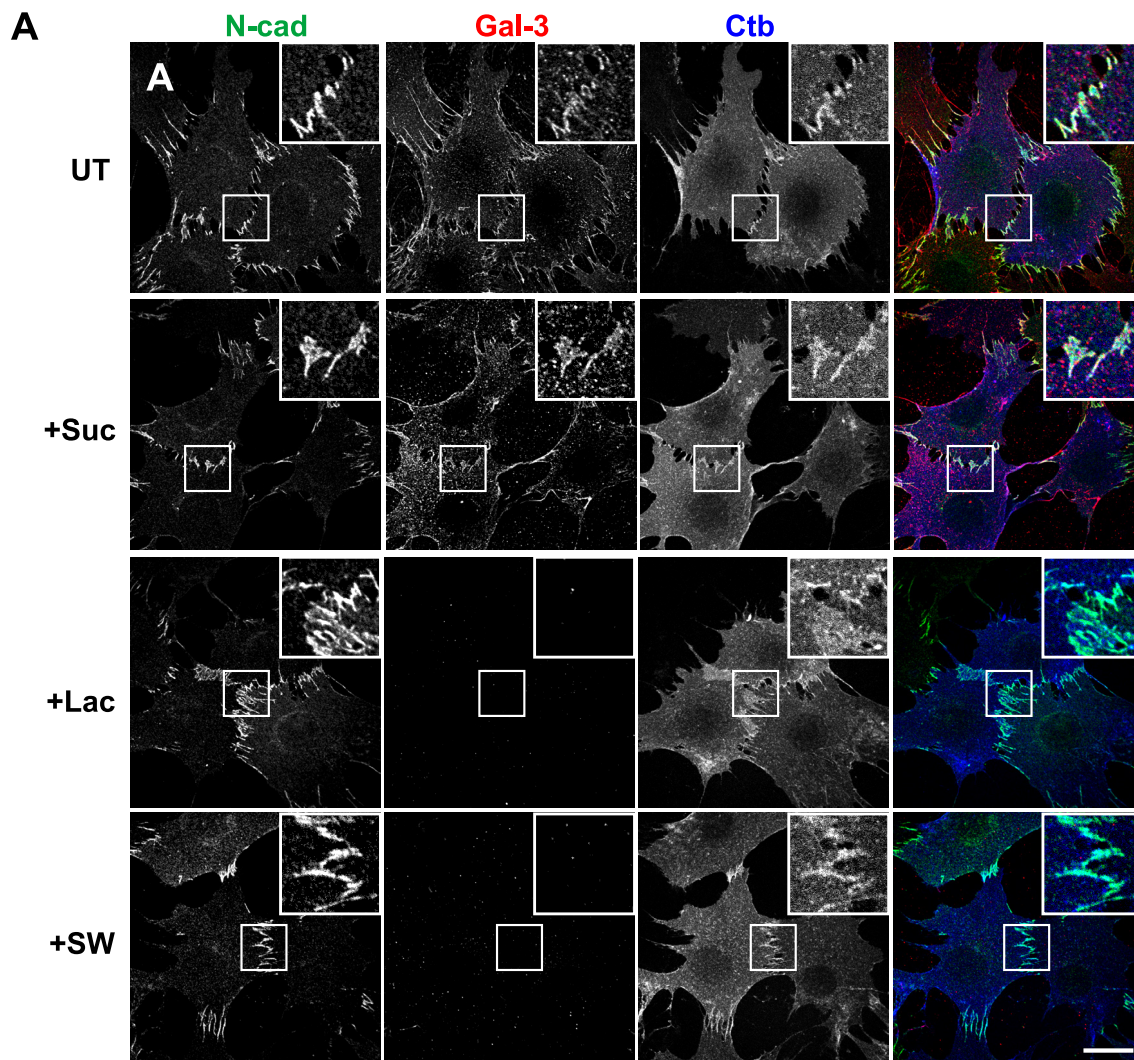
FIGURE 2. Galectin lattice decreases stability of cell-cell junctions. *A*, Mgat5$^{+/+}$ cells were transfected with nontargeting RNAi control (*siCtl*) or with siRNA targeting Gal-3 (*siGal-3*) 48 h before incubation with 1.5 mM EGTA for 25 min. After fixation, cells were stained for N-cadherin (*green*) and β-catenin (*red*). *B*, Mgat5$^{+/+}$ cells were untreated (*UT*) or treated with lactose (*+Lac*), sucrose (*+Suc*), or swainsonine (*+SW*). After 48 h, cells were incubated in low calcium medium (50 μM) for 8 min (*left*) or treated with 1.5 mM EGTA for 25 min (*right*) and then fixed. To quantify junction loss, images from all treatment conditions were acquired and thresholded equally, and the extent of colocalization (Pearson's coefficient) of N-cadherin and β-catenin per field was used as a measure of junctional stability. Quantifications of the average colocalization from eight fields containing 10–15 cells are presented ± S.E., *, $p < 0.05$, **, $p < 0.01$, ***, $p < 0.005$. Experiments were reproduced independently three times. *Bar*: 50 μm. *C*, Mgat5$^{+/+}$ cells were transfected with control (*siCtl*) or Gal-3 targeted (*siGal-3*) siRNA. After 48 h, cells were incubated with exogenous Gal-3 for 10 min before either the switch to low calcium medium (50 μM) or the addition of 1.5 mM EGTA, as indicated. Junction loss was quantified based on N-cadherin-β-catenin colocalization as described in *B*.

catenin, known to regulate cadherin stability and turnover (23, 35). We observed that the junctional mobility of a YFP-tagged N-cadherin mutated at the p120-catenin binding site (AAA-YFP (36)) was lower than that of N-cadherin-GFP mobility and was not affected by lactose treatment (Fig. 4, *A* and *B*, supplemental Table S1). p120-catenin siRNA reduced endogenous N-cadherin expression (supplemental Fig. S1), as reported previously (35). However, overexpressed N-cadherin-GFP still localized at cell-cell junctions where its mobility was markedly reduced when compared with control cells and not affected by lactose (Fig. 4*C*). Altogether, these results suggest that increased mobility of junctional N-cadherin upon recruitment to the galectin lattice is p120-catenin-dependent.

Galectin Lattice Regulation of Raft Composition—It has been proposed that p120-catenin regulates cell-cell junction formation and stability through recruitment of cadherins into raft microdomains (35). We have previously characterized the

DRM proteome of Mgat5$^{+/+}$ and Mgat5$^{-/-}$ cells and defined the impact of caveolae and caveolin-1 expression on the raft proteome of these cells (37). To specifically determine whether the galectin lattice affects raft protein composition, we performed quantitative proteomic analysis of DRMs from untreated Mgat5$^{+/+}$ cells and cells treated with lactose or sucrose (supplemental Fig. S3). The raft association of the vast majority of the more than 700 proteins detected was not significantly affected by disruption of the galectin lattice with lactose (Fig. 5*A*), and overall protein abundance ratios were highly similar for both lactose *versus* sucrose and lactose *versus* untreated samples (Fig. 5*B*). 181 proteins accumulated in rafts upon disruption of the galectin lattice for lactose *versus* control and 66 for lactose *versus* sucrose, whereas only four proteins were displaced from rafts by lactose treatment for either condition (Fig. 5*C*, supplemental Table S2). Therefore, the lattice predominantly inhibits protein traffic into rafts rather than facilitating

FIGURE 1. N-cadherin, Gal-3, and Ctb localize to cell-cell junctions. *A*, Mgat5$^{+/+}$ cells were untreated (*UT*) or treated for 48 h with 20 mM sucrose (*+Suc*), 20 mM lactose (*+Lac*), or 1 mM swainsonine (*+SW*) before incubation for 20 min at 4 °C with FITC-coupled Ctb (*blue*) and cyanine-3-coupled Gal-3 (*red*). Cells were fixed and stained for N-cadherin (*N-cad*) (*green*). *Insets* show accumulation of Gal-3 and Ctb at N-cadherin-positive cell-cell junctions. Gal-3 binding to the cells is reduced by lactose and swainsonine. *Bar*: 20 μm. *B*, Mgat5$^{+/+}$ cells were untreated or treated for 48 h with 20 mM sucrose, 20 mM lactose, or 1 mM swainsonine and then incubated or not with 1.5 mM EGTA (*+E*) for 1 h before incubation for 20 min at 4 °C with Gal-3. Cells were then incubated with 0.1 mg/ml DTSSP for 1 h at 4 °C. After quenching and cell lysis, cell extracts were submitted to N-cadherin immunoprecipitation (*IP Nc*). Pulldowns and total cell extracts (input) were analyzed by Western blot for N-cadherin (*Nc*) and Gal-3, and inputs were blotted for GAPDH as a loading control. *C*, Mgat5$^{+/+}$ cells were treated as described in *B* except that cells were incubated with GST-Gal-3 and immunoprecipitated with antibodies to β-catenin. 0.5 μg of purified Gal-3-GST were also loaded for Western blot analysis.

the exit of proteins. This is consistent with earlier work showing that the lattice recruits EGF receptors away from caveolin-1-positive raft domains (9). Proteins whose raft association increased upon disruption of the galectin lattice included Src (isoform 2), protein kinase Yes, and the β-adrenergic receptor

2a (Fig. 5A), suggesting that the raft localization of signaling proteins is affected by lattice integrity.

A number of cadherins and catenins, including N-cadherin (cadherin-2 or CDH-2), cadherin-11 (CDH-11, mesenchymal cadherin), β- and α-catenins and p120 (δ1-catenin, isoforms 1,
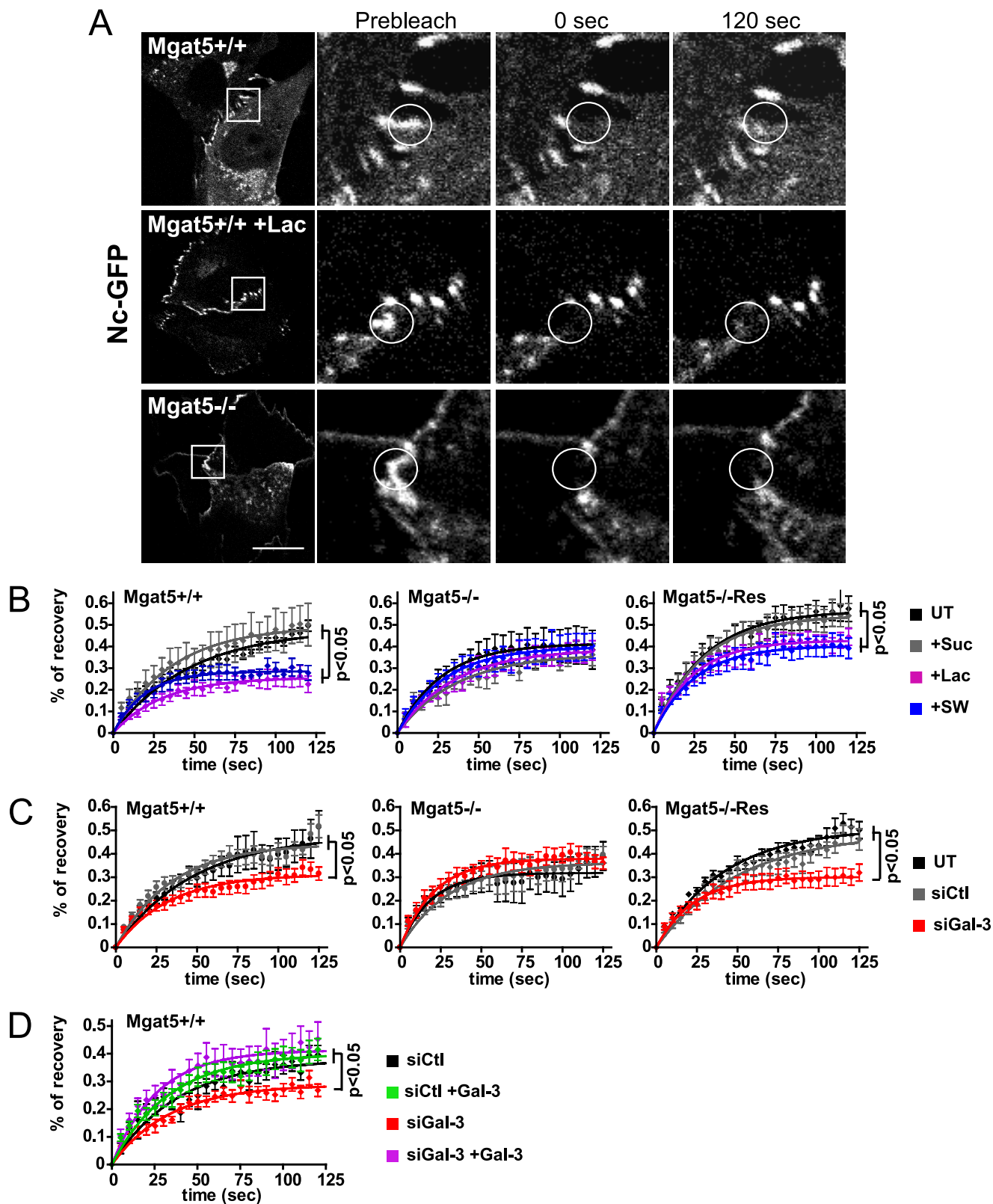
2, and 3) were detected in DRM fractions, as reported previously (33). However, their raft localization was similar with or without lattice disruption (Fig. 5*D*). This suggests that the galectin lattice regulates N-cadherin mobility and stability without affecting its distribution to raft microdomains.

Gal-3 Regulates Ctb Dynamics at Cell-Cell Junctions Independently from N-cadherin—GM1 is localized to cell-cell junctions with Gal-3 (Fig. 1*A*). If the galectin lattice binds and regulates glycoconjugates based on glycan affinity, GM1 mobility in adhesion junctions may also be affected. Cells were incubated with Ctb-FITC for only 5 min to limit endocytosis. In cell-cell junctions, Ctb FRAP was reduced upon lactose treatment or Gal-3 siRNA knockdown (Fig. 6, *A* and *B*, supplemental Table S1), whereas mobility of Ctb located in peripheral cellular regions, outside cell-cell contacts, was not affected by lactose (Fig. 6*C*). Swainsonine treatment, which results in loss of terminal *N*-glycans of glycoproteins but does not affect glycolipids, did not affect Ctb mobility in cell-cell junctions. However, treatment with both swainsonine and lactose did reduce Ctb mobility in cell-cell junctions (Fig. 6*B*). The ability of lactose to reduce junctional mobility of GM1 in swainsonine-treated cells suggests that Gal-3 might regulate GM1 dynamics independently of interactions with complex *N*-glycans. Moreover, the addition of extracellular Gal-3 significantly rescued the decrease of Ctb mobility at cell-cell junctions due to siRNA targeting Gal-3, supporting a role for the cell surface galectin lattice. Furthermore, p120-catenin knockdown did not affect junctional accumulation or lattice-dependent mobility of GM1 at cell-cell junctions (supplemental Fig. S4, *A* and *B*). This suggests that the lattice independently regulates junctional mobility of GM1 and N-cadherin.

To determine whether the galectin lattice regulates overall raft dynamics at cell-cell contacts, we assessed mobility of the unglycosylated raft protein flotillin-2-GFP, which is anchored to the inner plasma membrane through palmitoylation and myristoylation (38). Flotillin-2-GFP localizes to N-cadherin-positive junctions, and FRAP analysis of junctional flotillin-2-GFP revealed that disruption of the lattice did not significantly affect flotillin 2-GFP recovery (supplemental Fig. S4*C*). Therefore, the galectin lattice selectively regulates the dynamics of glycosylated binding partners, both lipid and protein, within cell-cell junction-associated domains.

DISCUSSION

Expression of Gal-3 and Mgat5 is closely associated with cancer progression (4, 39, 40), and interaction of Gal-3 with adhe-

sion and signaling receptors has been shown to promote tumor cell migration by clustering receptors in a lattice, which decreases their mobility (3, 4). Here we show that Gal-3 regulates the mobility of both glycoproteins and glycolipids within a particular plasma membrane domain, the cell-cell adhesion. Our data herein reveal that Gal-3 interacts directly with N-cadherin and that the integrity of the lattice is associated with reduced junctional stability upon calcium depletion as well as enhanced mobility of junctional N-cadherin. The Gal-3-dependent increase in N-cadherin mobility in cell-cell junctions requires both branched *N*-glycan ligands and extracellular Gal-3. N-cadherin mobility is reduced in Mgat5-deficient tumor cells or in cells treated with either swainsonine, which inhibits *N*-glycan branching, or lactose, which competes with extracellular Gal-3 binding. Reduced mobility of N-cadherin and Ctb in junctions due to Gal-3 siRNA knockdown is restored by the addition of extracellular Gal-3, defining a critical role for the cell surface lattice in both glycoprotein and glycolipid mobility at the cell-cell junction.

Lattice regulation of N-cadherin dynamics requires p120-catenin, indicating that recruitment to the lattice does not override p120 regulation of cadherin stability at cell surface (23, 24). Both disruption of the Gal-3 lattice and loss of p120 reduce the mobile fraction of N-cadherin. This suggests that they both function to enhance the mobile pool of N-cadherin in cell-cell junctions. Gal-3 promotes EGFR signaling (9), and EGF is known to induce p120 or β-catenin phosphorylation (28, 41). The lattice may therefore regulate N-cadherin mobility and cell-cell adhesion through the promotion of EGFR signaling as proposed for the regulation of E-cadherin by the Met receptor or VE-cadherin by VEGF receptor (42, 43). Another possibility is that the lattice decreases homotypic N-cadherin-N-cadherin interactions, which restrict junctional stability. Guo *et al.* (27, 28) reported that Mgat5 activity is inversely proportional to the stability of N-cadherin-mediated cell-cell adhesions. Branched *N*-glycans at three sites in the EC2 and EC3 ectodomains of N-cadherin were proposed to reduce homotypic N-cadherin interactions (27). Our data show that the Mgat5-dependent increase in N-cadherin dynamics at cell-cell junctions is mediated by Gal-3. Junctional stability is associated with a switch in cadherin conformation (44, 45), and it is possible that recruitment to the galectin lattice may impede clustering and alter N-cadherin conformation and recruitment of intracellular partners. Indeed, it was shown that E-cadherin hyperglycosylation results in immature and less stable cell adhesions due to

FIGURE 3. **The galectin lattice increases the N-cadherin-GFP mobile fraction at cell-cell junctions.** *A*, Mgat5$^{+/+}$ or Mgat5$^{-/-}$ cells were transfected with N-cadherin-GFP (*Nc-GFP*) and treated or not with lactose (+*Lac*) for 48 h before FRAP analysis (bleached zone is *circled*). *Boxed regions* are shown before bleach, immediately after bleach (0 s), and 120 s after bleach. *Bar*: 20 μm. *B*, FRAP analysis of N-cadherin-GFP was performed on Mgat5$^{+/+}$, Mgat5$^{-/-}$, or Mgat5$^{-/-\text{Res}}$ either untreated (*UT*) or following 48 h of sucrose (+*Suc*), lactose (+*Lac*), or swainsonine (+*SW*) treatment. 12–15 points were acquired from 10–15 cells, and the mean percentages of recovery of N-cadherin-GFP in individual cell-cell junctions are presented as a fitted curve according to the equation $Y = Y_{max} \times (1 - \exp(-0.69/X \times t_{1/2}))$; one of three independent experiments is represented here. A significant decrease in the plateau of the percentage of recovery is observed after lactose or swainsonine treatment in comparison with the sucrose or untreated cells (maximum recovery percentage values (Y_{max})) of untreated or sucrose-treated when compared with lactose or swainsonine treatment ($p < 0.05$). *C*, FRAP analysis of N-cadherin-GFP in Mgat5$^{+/+}$, Mgat5$^{-/-}$, and Mgat5$^{-/-\text{Res}}$ cells 48 h after transfection with control siRNA (*siCtl*) or siRNA against Gal-3 (*siGal-3*). Untreated cells or siCtl cells displayed a significant higher Y_{max} values in comparison with the siGal-3-treated cells. *D*, FRAP analysis of N-cadherin-GFP in Mgat5$^{+/+}$ cells transfected with control (*siCtl*) or Gal-3 targeting (*siGal-3*) siRNA. After 48 h, cells were incubated 10 min with Gal-3 before performing FRAP. Statistical analyzes revealed that the addition of Gal-3 did not affect the Y_{max} value of siCtl-treated cells but rescued the effect of siGal-3 treatment. Means of percentages of recovery of 12–15 individual cell-cell junctions are presented as fitted curves. Experiments were reproduced independently at least three times. See supplemental Table S1 for analysis of FRAP data from all experiments. Significant *p* values from Student's *t* test are indicated. *Error bars* indicate ± S.E.
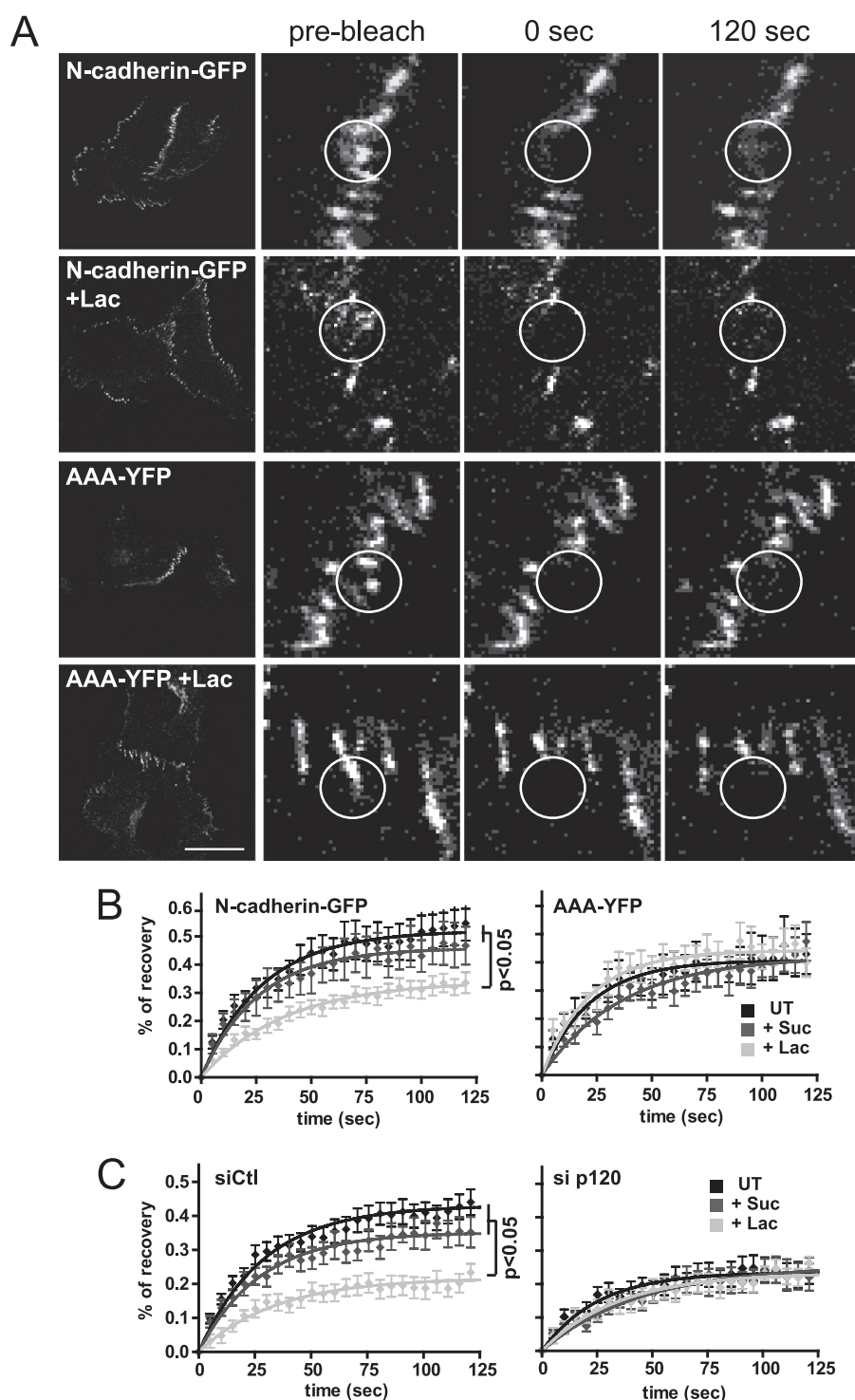
FIGURE 4. **Lattice-dependent N-cadherin-GFP mobility is p120-dependent.** *A*, Mgat5$^{+/+}$ cells were transfected with N-cadherin-GFP or the AAA-N-cadherin-YFP mutant (AAA-YFP) and grown in the presence of 20 mM sucrose or lactose (+*Lac*) for 48 h before performing FRAP at cell-cell junctions (*circles*). *Bar*: 20 μm. *B*, recovery curves and statistical analysis of FRAP experiments of sucrose- (+*Suc*) and lactose (+*Lac*)-treated N-cadherin-GFP or the AAA-N-cadherin-YFP transfected Mgat5$^{+/+}$ cells (*UT*, untreated). *C*, FRAP analysis of N-cadherin-GFP was performed on Mgat5$^{+/+}$ cells after transfection with control (*siCtl*) or p120-catenin targeted (*si p120*) siRNA and treatment with sucrose or lactose. The means of percentages of recovery of 12–15 individual cell-cell junctions are presented as fitted curves. Experiments were reproduced independently at least three times. See supplemental Table S1 for analysis of FRAP data from all experiments. Significant *p* values from Student's *t* test are indicated. *Error bars* indicate ± S.E.

increased spacing between dimers and differential recruitment of intracellular partners at cell-cell contacts (46, 47).

N-cadherin stabilization at cell-cell junctions has been shown to require raft microdomains (33). Gal-3, GM1, and N-cadherin colocalize at cell-cell junctions, and we also observed that cholesterol extraction with methyl-β-cyclodextrin disrupts cell-cell junctions (data not shown). We therefore performed proteomic analysis to determine the impact of lattice integrity on DRM protein composition. Interestingly, although most raft marker proteins, such as Cav1 and flotillin,
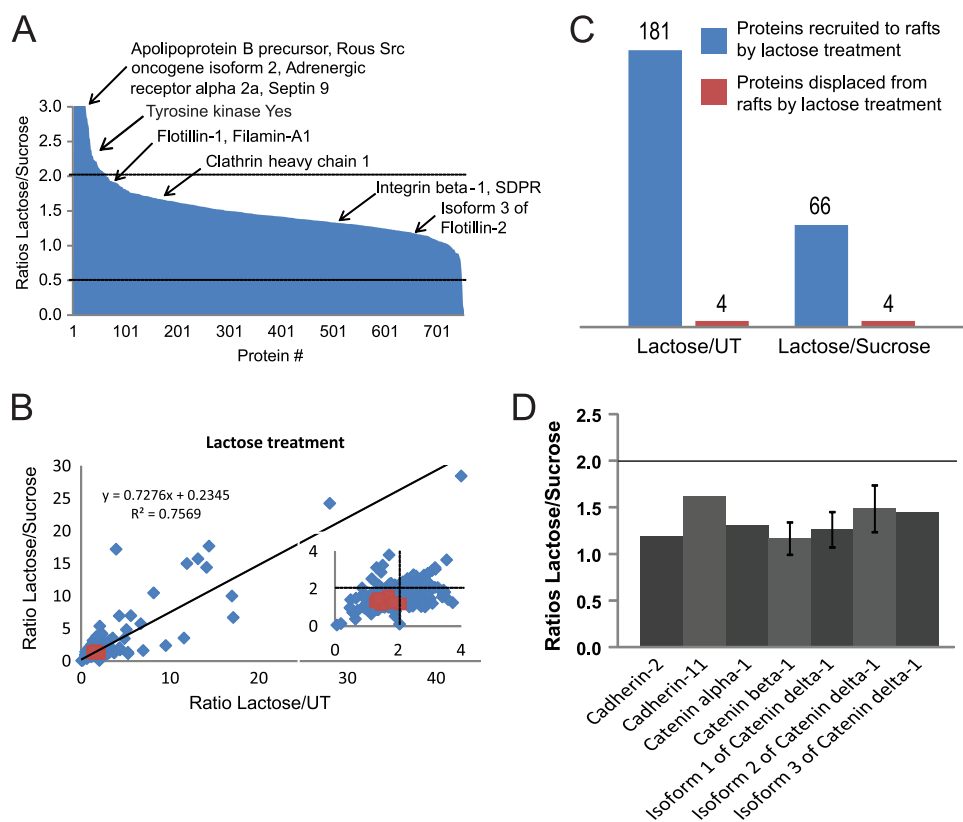
FIGURE 5. **Galectin lattice limits protein accumulation in rafts but not cadherins and catenins.** Triple SILAC was performed on Mgat5$^{+/+}$ cells growing in media supplemented with normal Lys and Arg (0/0), [^{2}H$_4$]Lys and [^{13}C$_6$]Arg (4/6), or [^{13}C$_6$^{15}N$_2$]Lys and [^{13}C$_6$^{15}N$_4$]Arg (8/10). 0/0 and 4/6 cells were treated with lactose and sucrose, respectively, with 8/10 as the untreated (*UT*) control. DRMs were extracted after combining equal amounts of protein from the 0/0, 4/6, and 8/10 lysates. *A*, the lactose/sucrose ratios for the more than 700 proteins identified are shown here, with specific proteins of interest highlighted. *SDPR*, serum deprivation factor. *B*, correlation plot of lactose/sucrose *versus* lactose/untreated ratios for all quantified proteins in DRMs. Proteins recruited to (*blue*) and displaced from (*red*) rafts by lactose treatment are indicated. *C*, histogram of the number of proteins recruited to (*blue*) and displaced from (*red*) rafts upon lactose treatment. *D*, lactose/sucrose ratios of identified cadherins and catenins fall between the cut-offs (2 and 0.5), indicating that their raft localization is not significantly affected by lactose treatment. *Error bars* indicate ± S.E.

were unchanged, lattice integrity was responsible for the predominant sequestration of proteins out of rafts with only four proteins found to be displaced from rafts upon lactose treatment. In contrast, using the same cell model and approach, we recently found that Mgat5$^{-/-}$ cells present reduced DRM protein content and that loss of Cav1 and caveolae expression in these cells reduces heterotrimeric G protein association with DRMs (37). We show here that lactose-mediated disruption of galectin lattice integrity does not affect G protein raft distribution (supplemental Table S2), suggesting that complex interplay between lattices, Cav1 scaffolds, and caveolae (48) impacts on protein recruitment to DRMs.

Proteins recruited to rafts upon lactose treatment include tyrosine kinase Yes and Src and the β-adrenergic receptor 2a that have been previously reported to be present in rafts (49–51). This suggests that the lattice may sequester signaling receptors and their effectors away from raft domains, as reported for EGFR interaction with Cav1 scaffolds and T cell receptor and CD45 in the immune synapse (9, 11). We did not observe any effect of lactose treatment on the DRM association of the multiple cadherins and catenins that were detected, including N-cadherin and p120-catenin. Although DRM preparations will contain rafts from the whole cell and not just the junction, the predominant localization of N-cadherin to cell-cell junctions where it colocalizes with the raft marker Ctb,

even in the presence of lactose (Fig. 1A), suggests that N-cadherin association with rafts in cell-cell junctions is not affected by disruption of the lattice. p120-catenin interaction with N-cadherin is required for recruitment of N-cadherin to raft microdomains, and functional N-cadherin-p120-catenin interactions occur within junctional raft domains (52). Our proteomics data suggest that raft localization of most junctional proteins, including N-cadherin, is independent of the lattice, but that their dynamics within junctions are regulated by Mgat5-dependent interaction with Gal-3.

Interestingly, the galectin lattice also enhances GM1 dynamics at cell-cell junctions (Fig. 6). Lattice enhancement of GM1 dynamics parallels that of N-cadherin, and both are specific for cell-cell junctions. Indeed, no effect of lattice disruption was observed for either N-cadherin or GM1 dynamics in cellular regions outside the junctions. p120-catenin knockdown disrupts lattice-dependent N-cadherin dynamics without affecting GM1 dynamics, and swainsonine, a specific inhibitor of *N*-glycan branching, has no effect on GM1 dynamics. As such, the ability of lactose and Gal-3 siRNA to reduce GM1 dynamics in cell-cell junctions of swainsonine-treated cells suggests that Gal-3 binds directly to glycolipids within the adherens junction. Indeed, although lactose completely removed Gal-3-GST, Gal-3-GST remained associated with the cells after swainsonine treatment (Fig. 1C).
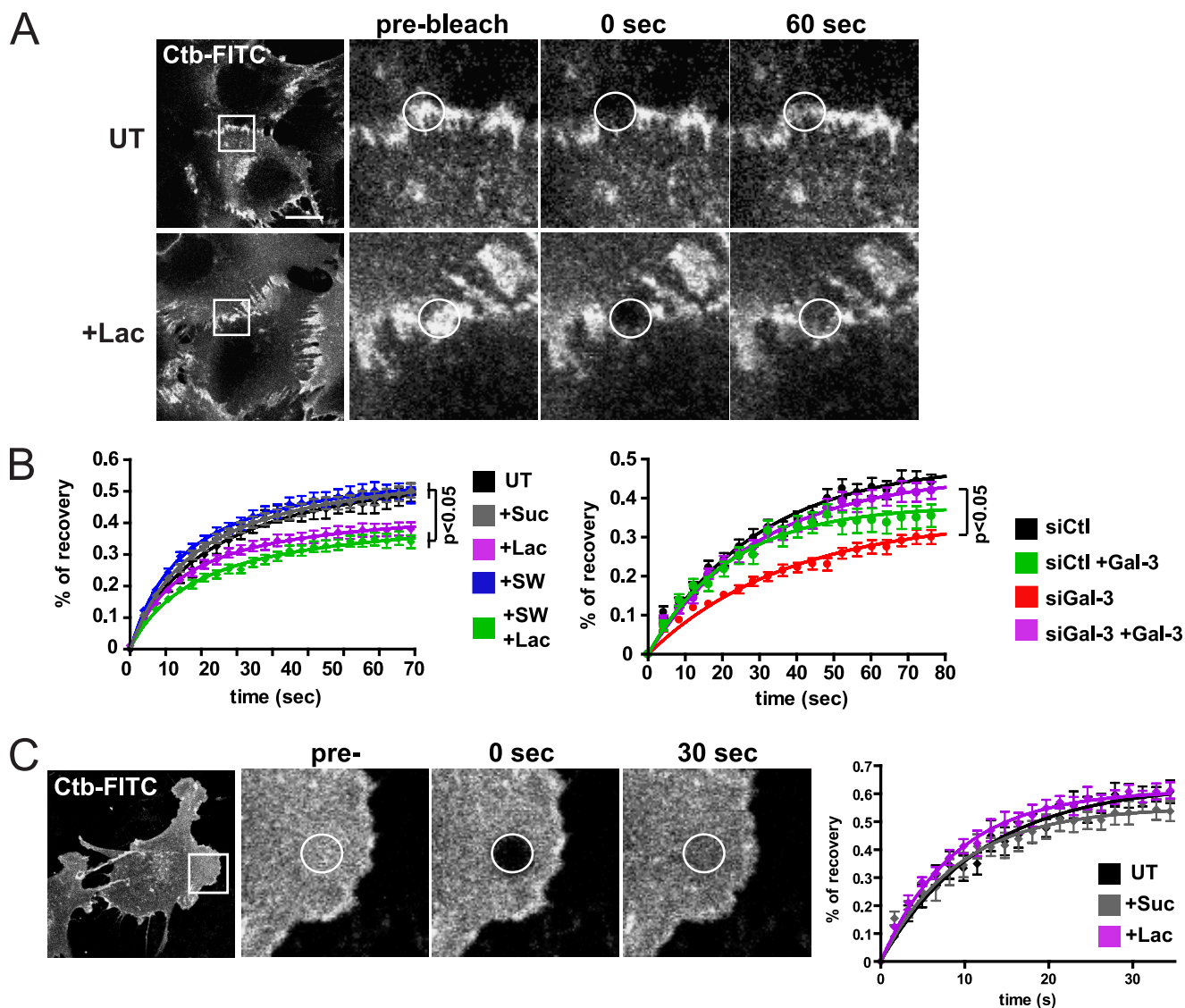
FIGURE 6. **Galectin lattice increases Ctb dynamics at cell-cell junctions.** *A*, Mgat5$^{+/+}$ cells were untreated (*UT*) or treated with 20 mM lactose (*+Lac*) for 48 h before incubation with Ctb-FITC at room temperature and FRAP of junction-associated regions (*circles*) at 30 °C. *B*, Mgat5$^{+/+}$ cells were untreated, treated with 20 mM sucrose (*+Suc*) or lactose, treated with 1 mM swainsonine (*+SW*) alone or in combination with lactose (*+Lac+SW*), or transfected with control siRNA (*siCtl*) or siRNA targeting Gal-3 (*siGal-3*). After 48 h, FRAP experiments were performed on Ctb-FITC located at cell-cell contacts. Cells were preincubated with purified Gal-3 where indicated. Quantification revealed higher Ctb mobility in cell-cell contacts in the presence of an intact galectin lattice. *C*, FRAP experiments were performed on Ctb-FITC in cellular regions not associated with a contact engaged zone (*circles*) of untreated cells or cells treated with 20 mM lactose or sucrose. The maximum percentage of recovery (Y_{max}) values derived from the FRAP showed no statistical difference between the untreated or sucrose-treated cells and the lactose-treated cells. The means of percentages of recovery of 30 individual cell-cell junctions are presented as fitted curves. Experiments were reproduced independently at least three times. See supplemental Table S1 for analysis of FRAP data from all experiments. Significant *p* values from Student's *t* test are indicated. *Bar*: 20 μm. *Error bars* indicate ± S.E.

Gal-3 is pluralistic in its ability to bind and cross-link glyco-conjugates, consistent with independent regulation of N-cadherin and GM1 dynamics within junction-associated raft domains and suggesting that Gal-3 may exchange between glycolipid and glycoprotein ligands. Indeed, our FRAP experiments revealed very different mobilities for N-cadherin and GM1 at cell-cell contacts, suggesting little physical interaction between the glycoprotein and GM1 glycolipid lattices at cell-cell junctions. Spatial considerations may account for this as glycolipid ligands are very close to the membrane and most glycoproteins extend well above the membrane, allowing independent levels of lattice organization.

Although the preferred and higher affinity substrate for galectins is branched *N*-glycans (1), galectins 1, 2, 3, 4, and 9 have been shown either to interact with glycolipids or to have been localized to rafts (19). Gal-3 colocalizes with Ctb in cell membranes and is detected in DRM fractions (53, 54). This study highlights for the first time independent and selective galectin regulation of glycoprotein and glycolipid raft components. Although we have focused on multivalent Gal-3, galectin-carbohydrate interactions have been proposed to form cell surface lattices with various geometries depending on valency (55). How interaction of different galectins with both glycoproteins and glycolipids contributes to lattice organization remains to be determined. Our work strongly supports the idea that Gal-3 lattice formation and turnover are critical membrane organizers at cell-cell contacts. Gal-3-dependent increase in N-cadherin dynamics at cell-cell junctions therefore represents

a mechanism whereby Gal-3 contributes to tumor cell motility and metastasis.

REFERENCES

1. Ahmad, N., Gabius, H. J., André, S., Kaltner, H., Sabesan, S., Roy, R., Liu, B., Macaluso, F., and Brewer, C. F. (2004) Galectin-3 precipitates as a pentamer with synthetic multivalent carbohydrates and forms heterogeneous cross-linked complexes. *J. Biol. Chem.* **279,** 10841–10847

2. Mehul, B., Bawumia, S., and Hughes, R. C. (1995) Cross-linking of galectin 3, a galactose-binding protein of mammalian cells, by tissue-type transglutaminase. *FEBS Lett.* **360,** 160–164

3. Nieminen, J., Kuno, A., Hirabayashi, J., and Sato, S. (2007) Visualization of galectin-3 oligomerization on the surface of neutrophils and endothelial cells using fluorescence resonance energy transfer. *J. Biol. Chem.* **282,** 1374–1383

4. Dennis, J. W., Nabi, I. R., and Demetriou, M. (2009) Metabolism, cell surface organization, and disease. *Cell* **139,** 1229–1241

5. Lau, K. S., Partridge, E. A., Grigorian, A., Silvescu, C. I., Reinhold, V. N., Demetriou, M., and Dennis, J. W. (2007) Complex *N*-glycan number and degree of branching cooperate to regulate cell proliferation and differentiation. *Cell* **129,** 123–134

6. Dennis, J. W., Laferté, S., Waghorne, C., Breitman, M. L., and Kerbel, R. (1987) β1–6 branching of Asn-linked oligosaccharides is directly associated with metastasis. *Science* **236,** 582–585

7. Raz, A., and Lotan, R. (1981) Lectin-like activities associated with human and murine neoplastic cells. *Cancer Res.* **41,** 3642–3647

8. Granovsky, M., Fata, J., Pawling, J., Muller, W. J., Khokha, R., and Dennis, J. W. (2000) Suppression of tumor growth and metastasis in Mgat5-deficient mice. *Nat. Med.* **6,** 306–312

9. Lajoie, P., Partridge, E. A., Guay, G., Goetz, J. G., Pawling, J., Lagana, A., Joshi, B., Dennis, J. W., and Nabi, I. R. (2007) Plasma membrane domain organization regulates EGFR signaling in tumor cells. *J. Cell Biol.* **179,** 341–356

10. Partridge, E. A., Le Roy, C., Di Guglielmo, G. M., Pawling, J., Cheung, P., Granovsky, M., Nabi, I. R., Wrana, J. L., and Dennis, J. W. (2004) Regulation of cytokine receptors by Golgi *N*-glycan processing and endocytosis. *Science* **306,** 120–124

11. Chen, I. J., Chen, H. L., and Demetriou, M. (2007) Lateral compartmentalization of T cell receptor versus CD45 by galectin-*N*-glycan binding and microfilaments coordinate basal and activation signaling. *J. Biol. Chem.* **282,** 35361–35372

12. Demetriou, M., Granovsky, M., Quaggin, S., and Dennis, J. W. (2001) Negative regulation of T-cell activation and autoimmunity by Mgat5 *N*-glycosylation. *Nature* **409,** 733–739

13. Grigorian, A., Lee, S. U., Tian, W., Chen, I. J., Gao, G., Mendelsohn, R., Dennis, J. W., and Demetriou, M. (2007) Control of T cell-mediated autoimmunity by metabolite flux to *N*-glycan biosynthesis. *J. Biol. Chem.* **282,** 20027–20035

14. Demotte, N., Stroobant, V., Courtoy, P. J., Van Der Smissen, P., Colau, D., Luescher, I. F., Hivroz, C., Nicaise, J., Squifflet, J. L., Mourad, M., Godelaine, D., Boon, T., and van der Bruggen, P. (2008) Restoring the association of the T cell receptor with CD8 reverses anergy in human tumor-infiltrating lymphocytes. *Immunity* **28,** 414–424

15. Demotte, N., Wieërs, G., Van Der Smissen, P., Moser, M., Schmidt, C., Thielemans, K., Squifflet, J. L., Weynand, B., Carrasco, J., Lurquin, C., Courtoy, P. J., and van der Bruggen, P. (2010) A galectin-3 ligand corrects the impaired function of human CD4 and CD8 tumor-infiltrating lymphocytes and favors tumor rejection in mice. *Cancer Res.* **70,** 7476–7488

16. Goetz, J. G., Joshi, B., Lajoie, P., Strugnell, S. S., Scudamore, T., Kojic, L. D., and Nabi, I. R. (2008) Concerted regulation of focal adhesion dynamics by galectin-3 and tyrosine-phosphorylated caveolin-1. *J. Cell Biol.* **180,** 1261–1275

17. Guo, H. B., Randolph, M., and Pierce, M. (2007) Inhibition of a specific *N*-glycosylation activity results in attenuation of breast carcinoma cell invasiveness-related phenotypes: inhibition of epidermal growth factor-induced dephosphorylation of focal adhesion kinase. *J. Biol. Chem.* **282,** 22150–22162

18. Lagana, A., Goetz, J. G., Cheung, P., Raz, A., Dennis, J. W., and Nabi, I. R. (2006) Galectin binding to Mgat5-modified *N*-glycans regulates fibronectin matrix remodeling in tumor cells. *Mol. Cell. Biol.* **26,** 3181–3193

19. Boscher, C., Dennis, J. W., and Nabi, I. R. (2011) Glycosylation, galectins, and cellular signaling. *Curr. Opin. Cell Biol.* **23,** 383–392

20. Yap, A. S., Brieher, W. M., Pruschy, M., and Gumbiner, B. M. (1997) Lateral clustering of the adhesive ectodomain: a fundamental determinant of cadherin function. *Curr. Biol.* **7,** 308–315

21. Vasioukhin, V., Bauer, C., Yin, M., and Fuchs, E. (2000) Directed actin polymerization is the driving force for epithelial cell-cell adhesion. *Cell* **100,** 209–219

22. Yamada, S., Pokutta, S., Drees, F., Weis, W. I., and Nelson, W. J. (2005) Deconstructing the cadherin-catenin-actin complex. *Cell* **123,** 889–901

23. Ireton, R. C., Davis, M. A., van Hengel, J., Mariner, D. J., Barnes, K., Thoreson, M. A., Anastasiadis, P. Z., Matrisian, L., Bundy, L. M., Sealy, L., Gilbert, B., van Roy, F., and Reynolds, A. B. (2002) A novel role for p120 catenin in E-cadherin function. *J. Cell Biol.* **159,** 465–476

24. Miyashita, Y., and Ozawa, M. (2007) Increased internalization of p120-uncoupled E-cadherin and a requirement for a dileucine motif in the cytoplasmic domain for endocytosis of the protein. *J. Biol. Chem.* **282,** 11540–11548

25. Thiery, J. P. (2002) Epithelial-mesenchymal transitions in tumor progression. *Nat. Rev. Cancer* **2,** 442–454

26. Hulit, J., Suyama, K., Chung, S., Keren, R., Agiostratidou, G., Shan, W., Dong, X., Williams, T. M., Lisanti, M. P., Knudsen, K., and Hazan, R. B. (2007) N-cadherin signaling potentiates mammary tumor metastasis via enhanced extracellular signal-regulated kinase activation. *Cancer Res.* **67,** 3106–3116

27. Guo, H. B., Johnson, H., Randolph, M., and Pierce, M. (2009) Regulation of homotypic cell-cell adhesion by branched *N*-glycosylation of N-cadherin extracellular EC2 and EC3 domains. *J. Biol. Chem.* **284,** 34986–34997

28. Guo, H. B., Lee, I., Kamar, M., and Pierce, M. (2003) *N*-Acetylglucosaminyltransferase V expression levels regulate cadherin-associated homotypic cell-cell adhesion and intracellular signaling pathways. *J. Biol. Chem.* **278,** 52412–52424

29. Panorchan, P., Thompson, M. S., Davis, K. J., Tseng, Y., Konstantopoulos, K., and Wirtz, D. (2006) Single-molecule analysis of cadherin-mediated cell-cell adhesion. *J. Cell Sci.* **119,** 66–74

30. Prakasam, A. K., Maruthamuthu, V., and Leckband, D. E. (2006) Similarities between heterophilic and homophilic cadherin adhesion. *Proc. Natl. Acad. Sci. U.S.A.* **103,** 15434–15439

31. Zheng, Y. Z., and Foster, L. J. (2009) Biochemical and proteomic approaches for the study of membrane microdomains. *J. Proteomics* **72,** 12–22

32. Foster, L. J., De Hoog, C. L., and Mann, M. (2003) Unbiased quantitative proteomics of lipid rafts reveals high specificity for signaling factors. *Proc. Natl. Acad. Sci. U.S.A.* **100,** 5813–5818

33. Causeret, M., Taulet, N., Comunale, F., Favard, C., and Gauthier-Rouvière, C. (2005) N-cadherin association with lipid rafts regulates its dynamic assembly at cell-cell junctions in C2C12 myoblasts. *Mol. Biol. Cell* **16,** 2168–2180

34. Volberg, T., Geiger, B., Kartenbeck, J., and Franke, W. W. (1986) Changes in membrane-microfilament interaction in intercellular adherens junctions upon removal of extracellular Ca^{2+} ions. *J. Cell Biol.* **102,** 1832–1842

35. Davis, M. A., Ireton, R. C., and Reynolds, A. B. (2003) A core function for p120-catenin in cadherin turnover. *J. Cell Biol.* **163,** 525–534

36. Thoumine, O., Lambert, M., Mège, R. M., and Choquet, D. (2006) Regulation of N-cadherin dynamics at neuronal contacts by ligand binding and cytoskeletal coupling. *Mol. Biol. Cell* **17,** 862–875

37. Zheng, Y. Z., Boscher, C., Inder, K. L., Fairbank, M., Loo, D., Hill, M. M., Nabi, I. R., and Foster, L. J. (2011) Differential impact of caveolae and

caveolin-1 scaffolds on the membrane raft proteome. *Mol. Cell. Proteomics* **10,** M110.007146

38. Neumann-Giesen, C., Falkenbach, B., Beicht, P., Claasen, S., Lüers, G., Stuermer, C. A., Herzog, V., and Tikkanen, R. (2004) Membrane and raft association of reggie-1/flotillin-2: role of myristoylation, palmitoylation, and oligomerization and induction of filopodia by overexpression. *Biochem. J.* **378,** 509–518

39. Chiu, C. G., Strugnell, S. S., Griffith, O. L., Jones, S. J., Gown, A. M., Walker, B., Nabi, I. R., and Wiseman, S. M. (2010) Diagnostic utility of galectin-3 in thyroid cancer. *Am. J. Pathol.* **176,** 2067–2081

40. Takenaka, Y., Fukumori, T., and Raz, A. (2004) Galectin-3 and metastasis. *Glycoconj. J.* **19,** 543–549

41. Mariner, D. J., Davis, M. A., and Reynolds, A. B. (2004) EGFR signaling to p120-catenin through phosphorylation at Tyr-228. *J. Cell Sci.* **117,** 1339–1350

42. Cozzolino, M., Stagni, V., Spinardi, L., Campioni, N., Fiorentini, C., Salvati, E., Alemà, S., and Salvatore, A. M. (2003) p120 catenin is required for growth factor-dependent cell motility and scattering in epithelial cells. *Mol. Biol. Cell* **14,** 1964–1977

43. Gavard, J., and Gutkind, J. S. (2006) VEGF controls endothelial cell permeability by promoting the β-arrestin-dependent endocytosis of VE-cadherin. *Nat. Cell Biol.* **8,** 1223–1234

44. Hong, S., Troyanovsky, R. B., and Troyanovsky, S. M. (2010) Spontaneous assembly and active disassembly balance adherens junction homeostasis. *Proc. Natl. Acad. Sci. U.S.A.* **107,** 3528–3533

45. Troyanovsky, R. B., Laur, O., and Troyanovsky, S. M. (2007) Stable and unstable cadherin dimers: mechanisms of formation and roles in cell adhesion. *Mol. Biol. Cell* **18,** 4343–4352

46. Liwosz, A., Lei, T., and Kukuruzinska, M. A. (2006) *N*-Glycosylation affects the molecular organization and stability of E-cadherin junctions. *J. Biol. Chem.* **281,** 23138–23149

47. Zhao, H., Liang, Y., Xu, Z., Wang, L., Zhou, F., Li, Z., Jin, J., Yang, Y., Fang, Z., Hu, Y., Zhang, L., Su, J., and Zha, X. (2008) *N*-Glycosylation affects the adhesive function of E-cadherin through modifying the composition of adherens junctions (AJs) in human breast carcinoma cell line MDA-MB-435. *J. Cell. Biochem.* **104,** 162–175

48. Lajoie, P., Goetz, J. G., Dennis, J. W., and Nabi, I. R. (2009) Lattices, rafts, and scaffolds: domain regulation of receptor signaling at the plasma membrane. *J. Cell Biol.* **185,** 381–385

49. DiPilato, L. M., and Zhang, J. (2009) The role of membrane microdomains in shaping β2-adrenergic receptor-mediated cAMP dynamics. *Mol. Biosyst* **5,** 832–837

50. Lu, S., Ouyang, M., Seong, J., Zhang, J., Chien, S., and Wang, Y. (2008) The spatiotemporal pattern of Src activation at lipid rafts revealed by diffusion-corrected FRET imaging. *PLoS computational biology* **4,** e1000127

51. Seong, J., Lu, S., Ouyang, M., Huang, H., Zhang, J., Frame, M. C., and Wang, Y. (2009) Visualization of Src activity at different compartments of the plasma membrane by FRET imaging. *Chem. Biol.* **16,** 48–57

52. Taulet, N., Comunale, F., Favard, C., Charrasse, S., Bodin, S., and Gauthier-Rouvière, C. (2009) N-cadherin/p120 catenin association at cell-cell contacts occurs in cholesterol-rich membrane domains and is required for RhoA activation and myogenesis. *J. Biol. Chem.* **284,** 23137–23145

53. Delacour, D., Greb, C., Koch, A., Salomonsson, E., Leffler, H., Le Bivic, A., and Jacob, R. (2007) Apical sorting by galectin-3-dependent glycoprotein clustering. *Traffic* **8,** 379–388

54. Hsu, D. K., Chernyavsky, A. I., Chen, H. Y., Yu, L., Grando, S. A., and Liu, F. T. (2009) Endogenous galectin-3 is localized in membrane lipid rafts and regulates migration of dendritic cells. *J. Invest Dermatol.* **129,** 573–583

55. Brewer, C. F., Miceli, M. C., and Baum, L. G. (2002) Clusters, bundles, arrays, and lattices: novel mechanisms for lectin-saccharide-mediated cellular interactions. *Curr. Opin. Struct. Biol.* **12,** 616–623